

Eco-Mobility-on-Demand Fleet Control with Ride-Sharing

Xianan Huang, Boqi Li, Huei Peng, Joshua A. Auld, Vadim O. Sokolov

Abstract—Shared Mobility-on-Demand using automated vehicles can reduce energy consumption and cost for future mobility. However, its full potential in energy saving has not been fully explored. An algorithm to minimize fleet fuel consumption while satisfying customers' travel time constraints is developed in this paper. Numerical simulations with realistic travel demand and route choice are performed, showing that if fuel consumption is not considered, the MOD service can increase fleet fuel consumption due to increased empty vehicle mileage. With fuel consumption as part of the cost function, we can reduce total fuel consumption by 12% while maintaining a high level of mobility service.

Index Terms—Connected Automated Vehicle, Mobility-on-Demand, Fuel Consumption, Data-driven Model, Ride-Sharing

I. INTRODUCTION

Ground transportation consumes 26.5% of the world energy in 2016 [1]. In 2014, 3.1 billion gallons of fuel and 6.9 billion hours of time are wasted due to congestion [2]. Mobility-on-demand (MOD) services such as Uber and Lyft have brought significant changes, especially in urban areas with dense population. When multiple passengers share the same vehicle (e.g., Lyft Line and UberPOOL), the number of vehicles parked and on the road will reduce, which in turn can reduce congestion and energy consumption. Intelligent transportation techniques enable smarter planners to reduce travel time and fuel [3], and the potential has not been fully explored.

A core piece for eco-routing algorithm is a robust fuel consumption model. Microscopic fuel consumption models have been studied [4–7], but for eco-routing, the fuel consumption of a large number of road sections needs to be evaluated, thus fast computation is also required. Macroscopic models [8–10] have also been studied to estimate fuel consumption but they typically did not consider heterogeneity in driving, resulting in the same fuel consumption for the same average speed, thus not appropriate for eco-routing. Mesoscopic models using road link average speed and grade are widely used for eco-routing [11, 12]. By considering link-based variables, they can address driving heterogeneity, thus are more accurate than macroscopic models. However, most of the existing mesoscopic models for eco-routing use parametric regression-based models [12, 13] or power balance models [14–16] and are not accurate enough due to the complexity of traffic

scenario and nonlinearity of vehicle powertrains. Advanced data-driven methods such as support vector machines (SVM) [17], neural networks (NN) [18] and multivariate adaptive regression spline (MARS) [19] were also studied, and many outperformed the traditional methods. Other strategies to estimate the energy cost for routing were also proposed, such as using probe vehicles of the same class [20] and generating synthetic speed profiles which are used as input to the well-studied microscopic models [21, 22].

Although eco-driving and eco-routing concepts have been proposed to reduce fuel consumption and emission at the operation level, as pointed out by a recent study on potential impact on fuel consumption of CAV technologies [23], the major cause for fuel consumption increase is the additional travel demand such as currently underserved population (2% ~ 40%), travel mode shift (~3.7%), and empty vehicle mileage (0%~11%). Thus, ride-sharing is proposed to reduce fuel consumption directly at the travel demand level [24] and has the potential to reduce vehicle mileage traveled by 12% [25]. However, currently the fleet assignment of MOD are either travel time oriented [26–31] or fleet sizing oriented [32–35], and the effect of fuel-saving is mainly due to reduced trips [36]. The full potential in fuel-saving by including trip-level techniques such as eco-routing or minimizing total fleet fuel consumption was not addressed in the literature.

Control of MOD fleet has been studied extensively to minimize customers' travel time. The fleet assignment problem falls in the category of dynamic Vehicle Routing Problem (VRP) [37] in the demand-vehicle network, which is a generalization of Traveling Salesman Problem (TSP) by allowing multiple vehicles to serve multiple customers. The problem is typically formulated as an integer programming problem. Several studies developed algorithms to find the exact solution [38–40]. However, due to the NP-hardness of VRP [41] and the large problem size, the centralized matching problem is hard to solve directly [42]. Thus, heuristic algorithms such as Genetic/Evolutionary algorithms combining insertion algorithm [43, 44] and bee colony optimization [45] are applied to find a suboptimal solution. Decomposition-based algorithms focus on reducing the problem size either spatially [46] or use Lagrange relaxation [47] to combine multiple smaller TSP into the master VRP, thus the solution process is accelerated due to the reduction in problem size and parallelization. Recently, [48] demonstrated that current travel demand for taxis in New York City could be fulfilled by a MOD fleet 15% the size of the existing fleet [27]. A data-driven approach is used to improve the quality of the solution by considering future demands [26]. [49] developed a simulation optimization (SO) framework using continuous approximation

Manuscript received XXX,XX, 2019. The research is supported by U.S. Department of Energy under the award DE-EE0007212.

X. Huang, B. Li, H. Peng are with the Department of Mechanical Engineering, University of Michigan, Ann Arbor, MI 48109, USA (e-mail: xnhuang@umich.edu, boqili@umich.edu, hpeng@umich.edu).

J. Auld is with the Energy Systems Division, Argonne National Laboratory, Lemont, IL, 60439, USA (e-mail: jauld@anl.gov).

V. Sokolov is with the Systems Engineering and Operations Research Department, George Mason University, Fairfax, VA, 22302, USA (e-mail: vsokolov@gmu.edu).

as a metamodel to improve computational efficiency. Other aspects of MOD systems were also explored. A privacy-preserving algorithm was developed [50] to protect the location information of passengers without a significant performance hit. Continuous approximation [51] is used to study the dynamics of the fleet and the influence of large fleet to congestion as well as the fleet routing problem in a congested network [29, 52]. The trade-off between the customers' travel time requirements and the system operator's cost is studied [53], where the system operator's cost is modeled as the time each vehicle spends in operation. Using fuel consumption as the cost, [54] solved green VRP without considering travel time constraint, thus cannot be applied to MOD system directly. As far as we know, none of the existing work considers fuel consumption when designing the controller, which is a core element in reducing the operation cost of the MOD service provider.

To include fuel consumption in the objective and integrate MOD fleet control with the recent eco-routing [3] concept, we developed a fleet control algorithm based on the work in [27] where the customers' wait time and travel delay time are modeled as constraints. We propose a MOD fleet control algorithm, Eco-MOD, to minimize the fleet operation cost (fuel consumption) while satisfying the customers' travel time constraints. In our study, travel demands generated by POLARIS [55], a mesoscopic agent-based transportation model, are calibrated with data from the Safety Pilot Model Deployment (SPMD) project [56] to generate the origins and the destinations of the customers. To evaluate the performance of Eco-MOD under realistic transportation environment, we developed a microscopic traffic simulator using Simulation of Urban Mobility (SUMO) [57] and performed a case study using the integrated model.

The main contributions of this work are: 1) a MOD fleet control algorithm which minimizing fleet fuel consumption directly while satisfying customer travel time constraints; 2) a simulation framework for MOD system with microscopic simulation from SUMO and demand generation from POLARIS; 3) demonstrating the importance of including fuel consumption in the optimization cost function to reduce fleet operating cost.

The rest of this paper is organized as follows: Section 2 presents the Bayesian nonparametric model used to estimate fuel consumption. Section 3 presents the formulation of fuel-efficient ride-sharing fleet optimization. Section 4 presents the simulation framework to evaluate the performance of the MOD fleet. Section 5 presents the simulation results. Conclusions and future work are given in Section 6.

II. FUEL CONSUMPTION ESTIMATION

A. Data Description

The real-world travel speed and grade trajectories are obtained from the Safety Pilot Model Deployment (SPMD) database [56]. The SPMD project's primary goal is to demonstrate connected vehicle technologies. It recorded naturalistic driving of up to 2,842 equipped vehicles, which is about 2% of the total vehicle population in Ann Arbor, Michigan for more than three years. As of April 2016, 56.2 million kilometers have been logged, making SPMD one of the

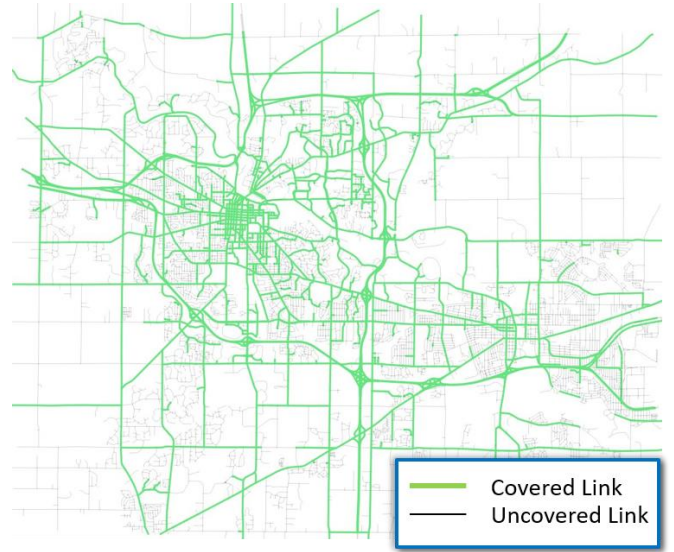


Fig. 1 Links with more than 100 trips each from the queried data

TABLE I KEY VEHICLE PARAMETERS FOR AUTONOMIE MICROSCOPIC SIMULATION

Vehicle Mass [kg]	1,246
Max Engine Power [kW]	178.7
Max Engine Efficiency [%]	36
Max Engine Speed [rad/s]	628.2
Idle Engine Speed [rad/s]	62.8
Transmission Gear Number	6
Fuel Type	Gasoline

largest naturalistic driving databases. The query criteria used for this paper are as follows:

- From May 2013 to October 2013
- Passenger cars
- Trip duration longer than 10 minutes
- Trip distance longer than 300 meters
- Trips in the Ann Arbor area: latitude between 42.18° and 42.34°, and longitude between -83.85° and -83.55°

The queried results contain 321,945 trips, which cover 3.7 million kilometers in 93,926 hours from 2,468 drivers. The data covers 9,745 of the 11,506 links in the Ann Arbor area, with 5,599 links covered by more than 100 trips. The links with more than 100 trips are shown in Fig. 1, which consist of major roads, minor roads, ramps, and highway sections. The speed and grade trajectories are used as the inputs to Autonomie [4], a microscopic fuel consumption model developed by the Argonne National Lab. The key vehicle parameters simulated are listed in TABLE I. We assume the representative vehicle for fuel consumption calculation is a mid-sized gasoline engine vehicle. Extending to other powertrain type is straightforward.

B. Single Link Fuel Consumption Model

We use the Autonomie simulation output as the ground truth to develop our fuel consumption model, which fits the average fuel consumption of all trips on all road links in Ann Arbor. In the modeling framework, we treat the speed limit as a categorical variable and fit a distinct set of model parameters for links with different speed limits. The fuel consumption model for each speed limit category is obtained using the Gaussian Mixture Regression model (GMR) technique. Instead

of modeling the regression function directly, GMR models the joint distribution of input and output variables and obtain the regression function through the conditional distribution of the output as functions of the inputs. By applying the Bayesian nonparametric formulation, the model has the flexibility required to model the complex nonlinear relations between fuel consumption and link/vehicle characteristics. Furthermore, the probabilistic nature allows to quantify uncertainty and account for the variance due to driving behavior. We denote the input variable as $X = [x_1, \dots, x_i, \dots, x_P] \in R^{N \times P}$, where $x_i \in R^N$ is individual input variable, N is the sample size, P is the number of input variables, and Y is the output variable, i.e., fuel consumption. Following the maximum likelihood formulation, the optimal model parameters are obtained by solving

$$\theta^* = \operatorname{argmax}_{\theta} \prod_{i=1}^N p(Y_i|X_i, \theta) \quad (1)$$

where $p(Y_i|X_i, \theta)$ is the conditional likelihood of Y_i on X_i and θ . The joint distribution of input and output can be factorized as

$$P(Y, X|\theta) = P(Y|X, \theta)P(X|\theta) \quad (2)$$

Since $P(X|\theta)$ depends only on the input variable and is independent of θ , maximizing the conditional likelihood of output is equivalent to maximizing the joint likelihood of input and output.

$$\theta^* = \operatorname{argmax}_{\theta} \prod_{i=1}^N P(Y_i, X_i|\theta) \quad (3)$$

In GMR, the joint distribution is modeled as a Gaussian mixture model (GMM).

$$f_{X,Y}(x, y) = \sum_{k=1}^K \pi_k f_{X,Y,k}(x, y) \quad (4)$$

$$f_{X,Y}(x, y) = \sum_{k=1}^K \pi_k f_{Y|X,k}(y|x) f_{X,k}(x) \quad (5)$$

where $f_{X,Y}(x, y)$ is the joint density function, π_k is the mixing coefficient for each component, $f_{X,Y,k}(x, y)$ is the joint density for each component, which follows a multivariate Gaussian distribution. Thus θ is the collection of mixing coefficients $\pi = (\pi_1, \dots, \pi_K)$, mean $\mu = (\mu_1, \dots, \mu_K)$ and covariance $\Sigma = (\Sigma_1, \dots, \Sigma_K)$ of the GMM. For each component of GMM, the conditional distribution of output on the input is Gaussian and can be presented in a closed form. The marginal distribution of X is

$$f_X(x) = \int f_{X,Y}(x, y) dy = \sum_{k=1}^K \pi_k f_{X,k}(x) \quad (6)$$

Thus, the conditional output density is

$$f_{Y|X}(y|x) = \sum_{k=1}^K w_k(x) f_{Y|X,k}(y|x) \quad (7)$$

where the posterior of component probability $w_k(x)$ is obtained from the marginal distribution of X .

$$w_k(x) = \frac{\pi_k f_{X,k}(x)}{\sum_{k=1}^K \pi_k f_{X,k}(x)} \quad (8)$$

The most popular approach to obtain parameters of the joint density function is to apply the Expectation-Maximization (EM) algorithm based on the maximum likelihood method. In the Expectation (E) step, the mixing coefficient is estimated using the mean and covariance of each component by calculating the posterior; in the Maximization (M) step, the mean and the covariance are estimated from the maximum likelihood method using the mixing coefficient from the E step.

To apply the EM algorithm, one needs to specify the component number of the GMM, which can be achieved through cross-validation. This can be achieved by randomly dividing the training dataset into validation dataset and new training dataset and evaluate the model performance with the validation dataset. However, since we construct independent models for different speed limits, specifying the component number for each speed limit through cross-validation can be time-consuming. Thus, instead of the EM algorithm, we adopt the Bayesian modeling framework, which models θ as hidden random variables and inference the expectation of θ from the data [58]. Multiple approaches can be used to solve the inference problem, including Markov Chain Monte Carlo (MCMC) and Variational Inference (VI). We apply the VI approach to get the expected values of the parameter. By applying the approximation to get tractable posterior, VI is faster and easier to scale to large data compared with MCMC [59]. The approach is summarized as follows. Denote $\tilde{X} = [X, Y]$ as joint of input and output, $Z = \{z_{nk}\}_{N \times K}$ as the indicator variable of the component for each data point, which is a binary variable. Thus, the likelihood of Z is given by

$$P(Z|\pi) = \prod_{n=1}^N \prod_{k=1}^K \pi_k^{z_{nk}} \quad (9)$$

The parameters are modeled with their corresponding conjugate priors, i.e., Dirichlet distribution for $\pi = (\pi_1, \dots, \pi_K)$ and Gaussian-Wishart distribution for mean and covariance of each component. By applying the conjugate priors, the posterior distributions are in the same probability distribution family as the prior distributions.

$$P(\pi) = \operatorname{Dir}(\pi|\alpha_0) = C(\alpha_0) \prod_{k=1}^K \pi_k^{\alpha_0-1} \quad (10)$$

$$P(\mu_k, \Sigma_k) = P(\mu_k|\Sigma_k)P(\Sigma_k) = N(\mu_k|m_0, \beta_0\Sigma_k)W(\Sigma_k^{-1}|W_0, v_0) \quad (11)$$

where $\alpha_0, m_0, \beta_0, W_0, v_0$ are hyperparameters. The hidden variables to inference include the indicator variable Z and the model parameters π, μ, Σ . The joint distribution is factorized as

$$P(\tilde{X}, Z, \pi, \mu, \Sigma) = P(\tilde{X}|Z, \pi, \mu, \Sigma)P(Z|\pi)P(\pi, \mu, \Sigma) \quad (12)$$

The VI approach uses a tractable (in this case, factorizable) posterior distribution of the hidden variables to approximate the original posterior distribution and minimize the Kullback-Leibler (KL) divergence between the true distribution and the approximated distribution. By applying the mean field approximation which assumes independence between Z and π , the approximate distribution is

$$q(Z, \pi, \mu, \Sigma) = q(Z)q(\pi, \mu, \Sigma) = q(Z)P(\pi)P(\mu, \Sigma) \quad (13)$$

It can be shown [58] that the stationary point of the KL divergence minimization problem satisfies

$$\ln q^*(Z) = E_{\pi, \mu, \Sigma}(\ln p(\tilde{X}, Z, \pi, \mu, \Sigma)) + \text{const} \quad (14)$$

$$\ln q^*(\pi, \mu, \Sigma) = E_Z(\ln p(\tilde{X}, Z, \pi, \mu, \Sigma)) + \text{const} \quad (15)$$

From the stationary point condition, we can update $q(Z)$ and $q(\pi, \mu, \Sigma)$ alternatively and iterate until convergence. The algorithm is initialized with hyperparameters of prior distributions. The approximated posterior of Z is first updated through (14), the mean and covariance are then obtained using the maximum likelihood method. For more details, refer to chapter 10 of [58]. The expectation of the mixing coefficient is

$$E(\pi_k) = \frac{\alpha_0 + N_k}{K\alpha_0 + N} \quad (16)$$

For a component with small sample size, $N_k \approx 0$, if a small hyperparameter α_0 is used, as sample size approaches infinity

$$\lim_{N \rightarrow \infty} E(\pi_k) = \lim_{N \rightarrow \infty} \frac{\alpha_0 + N_k}{K\alpha_0 + N} = 0 \quad (17)$$

Thus, a small hyperparameter for mixing coefficient can be used to remove the redundant components. In this way, we don't need to specify the component number for GMM. As the sample size increases, the influence of hyperparameters decreases. To see this, take the mixing coefficient as an example, since α_0 and K are finite, as N and N_k approaches infinity, the expectation is determined by the total sample size and the sample size for each component. Thus, the algorithm is less sensitive to tuned parameters compared with other algorithms such as SVM and neural networks.

The input variables we use for the fuel consumption model are listed in TABLE II. We include both linear and the 2nd order terms, including interaction terms of the input variables. Since we treat the speed limit as a categorical variable, with the assumption that the free-flow speed can be approximated by the speed limit, the average speed is also an indicator of the congestion status. Speed change and average grade are included to capture the kinetic and potential energy change.

TABLE II INPUT VARIABLES FOR FUEL CONSUMPTION MODEL

Motion Related	Average Speed [m/s]
	Speed Change [m/s]
Link Related	Average Grade [rad]
	Link Length [m]
	Posted Speed Limit [m/s]

III. TRAVEL DEMAND ASSIGNMENT

Our fleet control algorithm is based on the graph decomposition method proposed in [27]. The algorithm can solve the trip matching and routing problem for ride-sharing for thousands of vehicles and customers fast enough for real-world implementation. We further improve the algorithm to take knowledge of fuel consumption as the fleet operation cost.

We reproduce the work in [27] by assuming the road network is static and solving all optimal routes considering travel time and fuel consumption offline. Including dynamic road network information is considered as part of our future work. The trip assignment algorithm is based on a shareability graph. The graph is defined as an undirected graph with nodes defined as customers and vehicles. The constraints for each customer consist of wait time and delay time. Wait time is defined as the time between the customer travel request and time of pickup. Delay time is defined as the difference between planned travel time and the shortest travel time after pickup, which is from the minimum cost routing solution from origin to destination. An edge exists between two customers if a virtual vehicle can depart from the origin of one of the customers and fulfill the travel demands of both customers without violating travel time constraints. An edge exists between a vehicle and a customer if the demand can be served by the vehicle without violating travel time constraints. Then a necessary condition for a trip to be feasible is that the customers of the trip can form a clique with one vehicle present in the shareability network. A clique is a subgraph such that every node is connected to every other node within the same clique. It is noted that the cliques do not need

to be maximum in the shareability graph. The cliques in a graph can be found with the Bron-Kerbosch algorithm [60] with worst-case time complexity $O(dn3^{d/3})$ where n is the number of nodes and d is degeneracy of the graph, which is a measure of sparseness. In this way, instead of evaluating the cost for every possible combination of customers and vehicles, one can solve single-vehicle-multiple-customer problems modeled as TSP for every clique, a necessary condition for a trip to be feasible.

Trip scheduling for each clique is a traveling salesman problem with pickup and delivery. The problem can be solved with multiple algorithms. If the number of customers is small, (e.g., less than 5), the exact solution can be found by Dynamic Programming in less than 1 sec on a standard desktop computer. Heuristic-based algorithms such as T-share [61] can be used to find the solution if the problem size is large. In our numerical study, the vehicle capacity is set at 4, and Dynamic Programming is used to find the exact solution. The states are defined as

$\delta_t = [\delta_{1,t}^P, \dots, \delta_{i,t}^P, \dots, \delta_{N,t}^P, \delta_{1,t}^D, \dots, \delta_{i,t}^D, \dots, \delta_{N,t}^D] = [\delta_t^P, \delta_t^D]$ where $\delta_{i,t}^P$ and $\delta_{i,t}^D$ are indicator variable for pickup location and drop-off location of customer i at step t respectively, the value is 1 if the location has been visited and 0 otherwise. If two customers have the same pickup or drop-off locations, we assign individual variables for them, but define the transitional cost as 0. N is the total number of customers in the clique. The problem is to find the optimal trajectory to travel from the initial state, which is $\delta_0 = \{0\}_1^{2N}$, to the terminal state, which is $\delta_T = \{1\}_1^{2N}$. The constraints are

$$\delta_t^P - \delta_t^D \geq 0, \forall t \quad (18)$$

The constraint indicates that the drop-off locations are visited after the pickup locations of each customer.

$$\sum_i \delta_{i,t}^P - \delta_{i,t}^D \leq V_c, \forall t \quad (19)$$

where V_c is the capacity of the vehicle, indicating the number of customers onboard should not exceed the capacity of the vehicle. The continuity constraint is defined as

$$\|\delta_{t+1} - \delta_t\| = 1, \forall t \quad (20)$$

The constraint indicates that only 1 pickup/drop-off happens for each state. If the objective for fleet assignment is minimizing wait time and delay time of customers, the transitional cost is defined as

$$g(t, t+1) = \sum_i T_{t,t+1} \left((1 - \delta_{i,t}^P) + w_D (\delta_{i,t}^P - \delta_{i,t}^D) \right) \quad (21)$$

where $T_{t,t+1}$ is the travel time from location at t to $t+1$, w_D is the weighting parameter between wait time and on-vehicle travel time of the customer. If the objective of fleet assignment is minimizing the fuel consumption of fleet, the fuel consumption of traveling between locations associated with the states is used as the transitional cost. The objective of the TSP is minimizing the sum of the transitional costs from the initial state to the terminal state

$$J_{TSP} = \sum_{t=0}^{T-1} g(t, t+1) \quad (22)$$

where J_{TSP} is objective of the TSP step. A trip is feasible if the wait time and delay time constraints are satisfied for all customers in the clique. After all feasible trips were found

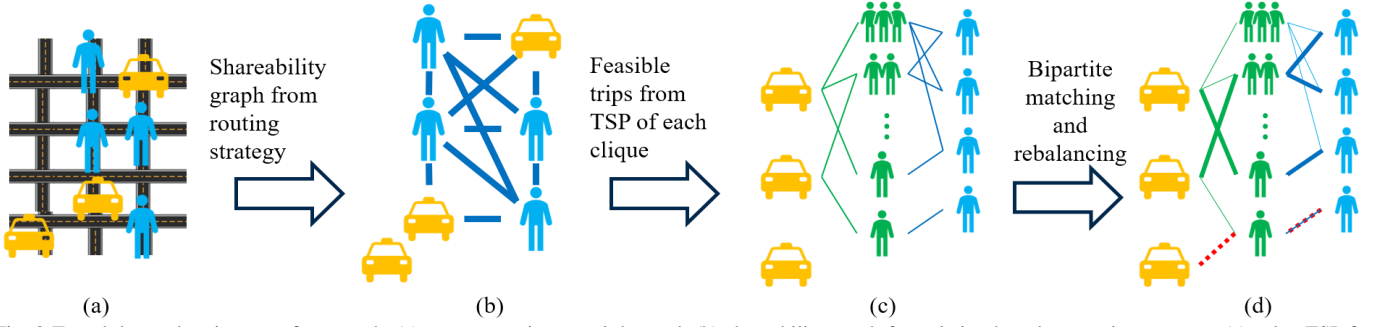


Fig. 2 Travel demand assignment framework: (a) system receive travel demand; (b) shareability graph formulation based on routing strategy; (c) solve TSP for each clique in the shareability graph to get all feasible trips; (d) assign trips to vehicles and assign ignored customers to idling vehicles for rebalancing, with thick solid line indicating feasible trip assignment and dashed line showing rebalancing assignment

through solving the TSP for all cliques, the optimal trip assignment problem can be formulated as a bipartite matching problem and solved through Integer Linear Programming (ILP).

The cost of a trip is denoted as c_t^i for trip i . The states of the system are δ_t which is the indicator variable for the trip/cliue and δ_c which is the indicator variable for the customer. If at an assignment instant, there are m feasible trips from the TSP step and n customers, then $\delta_t = \{\delta_t^i \in \{0,1\}, i \in \mathbb{N}, 1 \leq i \leq m\}$ and $\delta_c = \{\delta_c^i \in \{0,1\}, i \in \mathbb{N}, 1 \leq i \leq n\}$. δ_t^i is 1 if trip i is selected and δ_c^i is 1 if customer i is assigned. The objective function is

$$\sum_{i=1}^m c_t^i \delta_t^i + \sum_{i=1}^n D(1 - \delta_c^i), \quad (23)$$

where D is the penalty for unserved customers. In the original fleet control problem, a weighted sum of total wait time and delay time of each trip is used as cost, and in EcoMOD framework, the total fuel consumption is used as the cost. The constraint for the vehicle is that each vehicle can only serve one trip

$$\sum_{i=1}^m a_j^i \delta_t^i \leq 1, \forall j, \quad (24)$$

where a_j^i is the indicator variable for vehicle j and trip i , $a_j^i = 1$ if vehicle j can serve trip i . The constraint for the customer is that a customer is either assigned or ignored

$$\sum_{i=1}^m b_j^i \delta_t^i + (1 - \delta_c^j) = 1, \forall j, \quad (25)$$

where b_j^i is the indicator variable for customer j and trip i , $b_j^i = 1$ if customer j can be served by trip i . With linear constraints and the objective function, the trip assignment problem is an integer linear programming. Since all candidate trips are feasible from construction, the travel time constraints are satisfied. For online optimization, we follow [27] to keep a pool of customers, and a customer is removed from the pool if it's picked up by vehicle or cannot be served within the time constraint. If a customer is ignored, a vehicle from the idling fleet is assigned to serve the customer with the minimum wait time as the objective. The framework to solve the fleet control problem is summarized in Fig. 2. Gurobi [62] is used to find the solution of ILP. The optimization problem is solved every assignment interval reacting to new travel requests.

IV. TRAFFIC SIMULATOR

POLARIS is an agent-based traffic simulation software developed by the Argonne National Lab [55] focusing on travel demand and mesoscopic traffic simulations. Travel demand is generated using the ADAPTS (Agent-based Dynamic Activity Planning and Travel Scheduling) model in POLARIS, which formulates the activity planning of individuals as a dynamic model [63]. The demand model is calibrated by the Argonne National Lab using the dataset from the Safety Pilot Model Deployment project using real data from the city of Ann Arbor. The data is aggregated over 5 months, from May 2013 to October 2013. However, as a mesoscopic simulator, POLARIS's ability to simulate individual vehicle's dynamics is limited. Thus, POLARIS is used as travel demand generator, with which 110,000 trips are generated from 17:00 to 19:00 and a microscopic transportation simulator, Simulation of Urban Mobility (SUMO) [57] is used for verification and to generate individual vehicle trajectories with speed changes. The demand generated by POLARIS is calibrated to recreate the observed average link speed from SPMD by treating it as prior in the calibration process.

SUMO is an open-source microscopic traffic simulator with the ability to generate realistic route choice and speed profile. In the simulations, the background traffic is calibrated using data from SPMD using demand generated by POLARIS as prior, and a random subset of demands are assumed to be served by the MOD fleet. We assume the ratio of the MOD customers to the total demand is fixed. The fleet size is assumed to be fixed and ride-sharing is allowed. A fleet controller implemented in Matlab is used to control the route choice of the MOD vehicles using the TraCI4Matlab package [64]. The simulation framework is summarized in Fig. 3.

The model is calibrated using the measured average speed from SPMD. In the calibration process, we focus on route

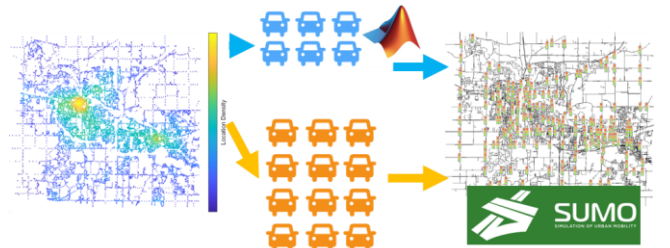


Fig. 3 Transportation Simulation Framework

choice and travel demand distribution. Demand generated by POLARIS is used as prior for demand distribution estimation from measured average speed. The microscopic model parameters including the car-following model and the lane-change model are obtained from [65]. In the simulation framework, we only consider passenger cars. To estimate demand distribution given average speed measurement, we use a data-driven approach to model the relation between vehicle density and the average travel speed for links in SUMO, which is used to estimate expected flow rate at each link given the measured average speed. A second-order polynomial is used when the density is below critical density for simplicity. When the vehicle density is higher than the critical density $\rho_{critical}$, we assume the average speed is a constant.

$$\bar{v}_n = \begin{cases} \epsilon & \rho \geq \rho_{critical} \\ \alpha_2 \rho^2 + \alpha_1 \rho + \alpha_0 & otherwise \end{cases}, \quad (26)$$

where \bar{v}_n is normalized average speed, defined as average speed normalized by the free-flow speed. ρ is the vehicle density at each link, ϵ is normalized average speed when the vehicle density is higher than the critical density. Flow rate, vehicle density and average follow are related by

$$q = N\rho\bar{v}, \quad (27)$$

where \bar{v} is the average speed, q is flow rate, and N is the number of lanes. Given measured average speed from SPMD, the flow rate \widehat{q}_{SPMD} is estimated. To estimate travel demand and route choice, we assume the drivers follow the shortest distance route, empirical shortest time route, or real-time shortest time route. Under the assumption that the system has reached steady state, given flow rate between origin-destination pair q_{od} , the flow rate for each link is given by

$$q_l = \sum_k (q_{od}^{k,d} i_{od,d}^{k,l} + q_{od}^{k,t} i_{od,t}^{k,l}), \quad (28)$$

where $i_{od,d}^{k,l}$ and $i_{od,t}^{k,l}$ are indicator variables to show that link l is used by OD pair k following shortest distance route and empirical shortest time route respectively, $q_{od}^{k,d}$ and $q_{od}^{k,t}$ are the flow rate for OD pair k following the shortest distance route and empirical shortest time route, respectively. The OD flow is modeled using the partitioned road network from [66].

$$q_{od}^k = q_{od}^{k,d} + q_{od}^{k,t}, \quad (29)$$

The objective of the calibration is to minimize the difference between the simulated flow rate and the estimated flow rate using the data-driven model from SPMD.

$$\min_{q_{od}^{k,t}, q_{od}^{k,d}} \sum_l \|q_l - \widehat{q}_{l,SPMD}\|^2 + \sum_k \psi \|q_{od}^k - q_{od,POLARIS}^k\|^2, \quad (30)$$

where $\widehat{q}_{l,SPMD}$ is estimated link flow rate from SPMD, $q_{od,POLARIS}^k$ is OD flow rate from POLARIS. ψ is the weighting parameter between flow rate approximation and the regularization term using POLARIS. Given the assumption that OD flow rate follows Gaussian distribution, the objective function is equivalent to the maximum-a-posterior estimation of OD flow rate using POLARIS OD flow rate as prior. Assuming the total flow rate follows the total flow rate generated by POLARIS, we have the constraint

$$\sum_k q_{od}^k = \sum_k q_{od,POLARIS}^k, \quad (31)$$

The objective function is quadratic in OD flow rate and the constraints are linear, thus the optimization problem is convex. The quadratic program is solved using Gurobi. Shortest distance route and shortest time route are generated offline, and the percentage of drivers following the shortest distance in each OD flow is obtained by solving (30). To generate the empirical shortest time route, we use measured average speed, and for links with inadequate data, we assume the average flow speed is equal to the posted speed limit. We assume that the drivers follow real-time shortest time routes are uniformly distributed in the road network and the ratio is estimated by simulation. Also, we assume that the average speed on each link is normally distributed. The real-time routing ratio with the maximum likelihood of the average speed is selected as the optimum value. If variances of average speed distribution are equal for all links in the network, this is equivalent to minimize the squared error between simulated and measured mean value of average speed.

V. ECO-MOD COST CONFIGURATIONS

Two levels of strategies can be used by the MOD fleet to reduce fuel consumption. At the trip assignment level, the objective function for the fleet assignment of the feasible trips can be the total fleet fuel consumption instead of the sum of individual's wait time and delay time as defined in the original fleet assignment problem [27]. However, for the assignment of the rebalance fleet, where the main objective is to serve the customers whose travel demand cannot be satisfied within the travel time constraints, we use their travel time as t

The objective function when assigning the idling vehicles to the rebalancing trips. At the trip execution level, the routing strategy can be either shortest-time routing or eco-routing, and the corresponding routing cost is applied for the trip assignment. To assess the fuel-saving benefit of the two levels, nine test configurations are defined based on combinations of the cost function and the routing strategy. In all configurations, the rebalancing trips are assigned to minimize the travel time under the corresponding routing policy. The configurations are summarized in TABLE III, where the assignment of the feasible trips is denoted as assignment, and the assignment of the reactive rebalance trips is denoted as rebalance. Configuration 9 is the baseline where personal vehicles are used, where the routing strategy is from the calibration of the traffic simulator.

TABLE III MOD FLEET ASSIGNMENT STRATEGY CONFIGURATION SUMMARY

	Assignment Cost	Assignment Routing Strategy	Rebalance Routing Strategy
1	Trip Time	Fastest Routing	Fastest Routing
2	Trip Time	Fastest / Eco Routing	Fastest / Eco Routing
3	Trip Time	Eco Routing	Fastest Routing
4	Trip Time	Eco Routing	Eco Routing
5	Fleet Fuel	Fastest Routing	Fastest Routing
6	Fleet Fuel	Fastest / Eco Routing	Fastest / Eco Routing
7	Fleet Fuel	Eco Routing	Fastest Routing
8	Fleet Fuel	Eco Routing	Eco Routing
9	-	Shorest Distance/ Fastest	-

As shown in TABLE III, configurations 1-4 weighs more on time, while configurations 5-8 weighs more on fuel consumption. The travel time requirement of customers are addressed as constraints and are satisfied by the graph decomposition based formulation. The configurations are compared with the baseline (configuration 9) that the personal vehicles are used for the trip. The routing strategies of configurations 2 and 6 depends on the occupancy of the vehicles. If the vehicle is occupied, then the shortest time route is used. Otherwise, the eco route is used.

VI. RESULTS AND DISCUSSION

In the following, simulation results from the SUMO model are presented. First, we verify that our calibrated simulator can recreate average speed at evening rush hour of Ann Arbor, and then the model is used to estimate the effect of eco-MOD at city-scale. Then the fleet size required to serve 4% of the total travel demands for Ann Arbor from 17:00 to 19:00 is estimated. Due to the approximations made by the models, a parametric study of fleet size is performed using the calibrated traffic simulator to evaluate the system performance. Finally, simulation results of eco-MOD using the configurations from section V are presented.

A. Fuel Consumption Model Performance

The fuel consumption model performance is measured using the coefficient of determination (R^2) and the mean absolute percent error (MAPE). Since the objective of the model is to predict the conditional expectation of fuel consumption on motion and link variables, we compare the model output with the conditional expectation of fuel consumption given the average speed and speed change. To get the conditional expectation, we fit individual GMR for each link with more than 100 trips.

Through the model of individual links, we can get the conditional expectation of fuel consumption as the complete model described in Section II. We randomly selected 70% of links as the training dataset and the rest as the testing dataset. We use the conditional expected fuel consumption of test dataset as the ground truth. We compared our model with (i) the average speed model [13] as shown in (32), (ii) the power balance model which is the foundation of MOVES [8] as shown in (33), and (iii) the neural network model.

$$\ln(f/t) = \beta_0 + \beta_1 v + \beta_2 v^2 + \beta_3 v^3 + \beta_4 v^4 + \beta_5 s \quad (32)$$

$$f = \beta_0 vt + \beta_1 vat + \beta_2 svt + \beta_3 v^3 t \quad (33)$$

where f is the expected link fuel consumption, t is average link travel time, v is average link travel speed, a is average link acceleration, s is average link grade, β_1, \dots, β_5 are the model parameters of the corresponding model. Parameters of the benchmark models are also estimated from the training dataset. For the neural network model, we used a two-layer structure with two fully connected layers and sigmoid function as the activation function for the output of layer 1. The relative error of the models are shown in Fig. 4 and model performance metrics are summarized in TABLE IV.

From the histogram and performance metrics, we can see that both our GMR model and the neural network model have superior performance over the other two models. Neural

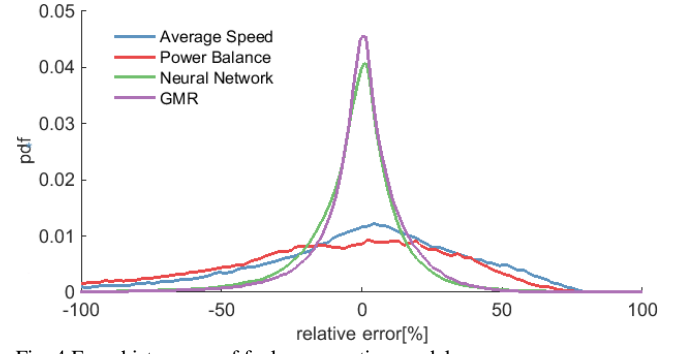


Fig. 4 Error histograms of fuel consumption models

TABLE IV PERFORMANCE OF FUEL CONSUMPTION MODELS

Model	R^2	MAPE [%]
Average speed model	0.77	37.63
Power balance model	0.86	46.22
Neural Network	0.98	15.60
GMR	0.98	10.08

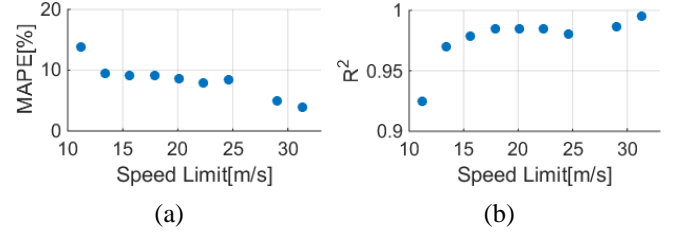


Fig. 5 Model performance for different speed limits: (a) MAPE; (b) R^2

network models with well-tuned structure and parameters including number and structure of layers, type of activation functions, and the number of hidden variables have the potential to achieve similar or better performance than our GMR model. However, the main advantage of our model is that it is nonparametric while many parameters need to be tuned for neural network models. Also, the final form of our model is simpler compared with the neural network models. Besides that, with the Bayesian nonparametric formulation, the uncertainty of our model parameters can be quantified in closed form using the posterior distribution, while the uncertainty quantification of the neural network model is still under investigation [67, 68].

The GMR model performance for links with different speed limits are shown in Fig. 5. The worst performance happens at links with low speed limit 11.18 m/s (25 mph) with MAPE is 13.78%. The MAPE for links with higher speed limits is less than 10%. The reason, we believe, is that links with lower speed limit contain more speed and traffic variations. Also, at low speed and low torque, the engine fuel consumption is highly nonlinear with power, while for high power operation, the fuel consumption – power relationship is more linear.

B. Traffic Simulator Calibration

Assuming microscopic driving behavior by using parameters from [65], the demand distribution and route choice are calibrated using data from SPMD. Links with more than 100 events are used for calibration. The marginal distribution of origins and destinations are shown in Fig. 6 and Fig. 7, with high density indicated by yellow and low density indicated by blue. Measured and simulated average speed normalized using

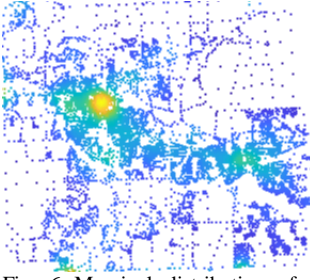


Fig. 6 Marginal distribution of generated trip origins during weekday evening rush hour

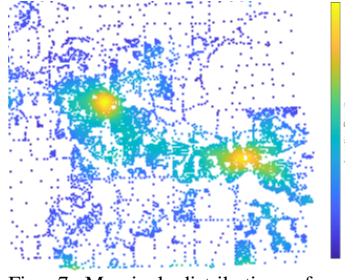


Fig. 7 Marginal distribution of generated trip destinations during weekday evening rush hour

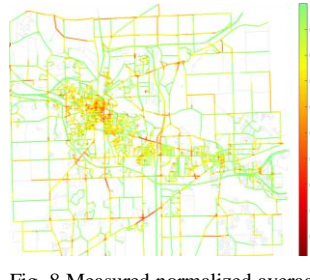


Fig. 8 Measured normalized average speed from 17:00 to 17:30

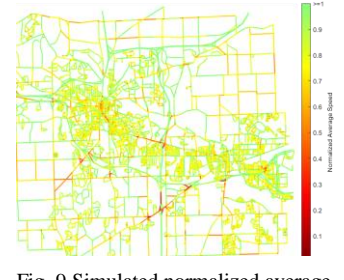


Fig. 9 Simulated normalized average speed from 17:00 to 17:30

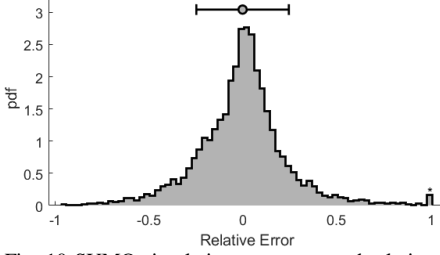


Fig. 10 SUMO simulation average speed relative error distribution

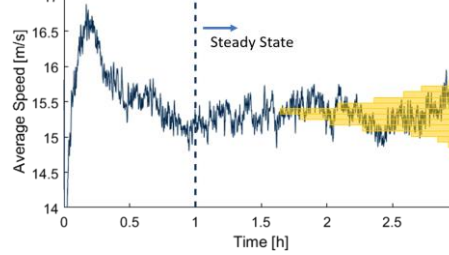


Fig. 11 SUMO simulated network average speed

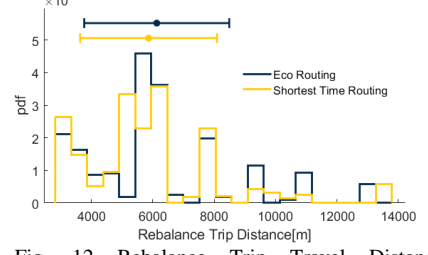


Fig. 12 Rebalance Trip Travel Distance Distribution

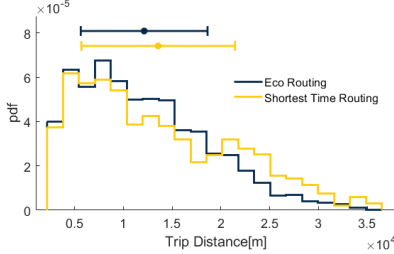


Fig. 13 Generated Trip Travel Distance Distribution

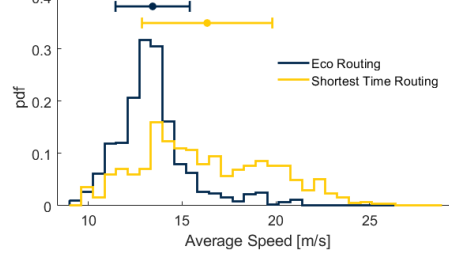


Fig. 14 Average Speed Distribution of Partition Pairs

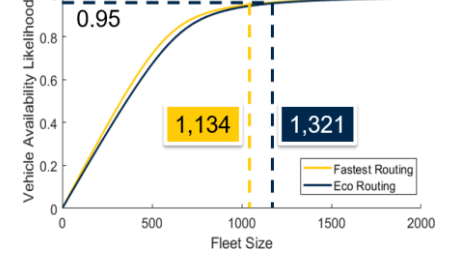


Fig. 15 Vehicle Availability Estimated Using Queuing Network Model

posted speed limit from 17:00 to 17:30 are shown in Fig. 8 and Fig. 9 respectively, with low speed indicated by red and high speed indicated by green, and links without enough data are shown in light gray. The relative error distribution is shown in Fig. 10, with mean relative error equals -1% and the standard deviation equals 25%. As shown in Fig. 8 and Fig. 9, the simulation results show less congestion in the downtown area, possibly due to our assumption that the flow is only generated by passenger cars, our ability to simulate pedestrians and public transits in the downtown is limited. As a result, the extended stops due to pedestrian crossings or bus stops are not captured in our model. However, developing a detailed high fidelity traffic simulator is out of the scope of this study and is left for future work. 150,457 trips are generated from 17:00 to 19:00.

When using the simulator to evaluate the Eco-MOD framework, we simulate from 16:00 to 19:00. Only background traffic is generated in the first hour to reach the steady-state of the traffic network. The MOD fleet starts to be deployed in the second hour to reach the steady-state of service fleet. The data from the third hour is used to evaluate the efficiency of the system. The average speed of running vehicles of background traffic simulation is shown in Fig. 11 with the histogram of the average speed at the steady-state shown in yellow. As shown in the figure, the system reaches steady-state within the first hour, and the standard deviation of average speed is 0.18 m/s at the steady-state.

C. Fleet Size Estimation

To estimate the size of the fleet required to serve the travel demands, we apply the distance-based approach from [69] and the queuing network approach from [70]. We assume that each vehicle only serves one customer. Thus the estimation is conservative. However, this doesn't ensure that all travel demands can be served within their time constraints using the algorithm described in section III. In the algorithm, the idling vehicles are sent to serve the customers whose time constraints cannot be satisfied by the assignment trips, while [70] assumes customers cannot be served will leave the system instead of waiting for the available vehicle and [69] doesn't take the travel time into consideration. Thus a parametric study is performed to analyze the influence of the fleet size on system performance.

When applying the methods to estimate fleet size, the average travel speed and distance are estimated using the shortest time routing and eco-routing. The distributions of the network statistics required to estimate the fleet size using the distance-based approach are shown from Fig. 12 to Fig. 14. The estimated minimum fleet size for eco-routing is 1,176, and 1,039 for the shortest time routing to serve 4% of the total travel demand from 17:00 to 19:00. Since the approach only addresses the minimum fleet size problem using travel distance and average speed, the wait time of customers can be long [69]. Therefore, the distance-based approach can be used as a lower bound estimation if there is no shared ride.

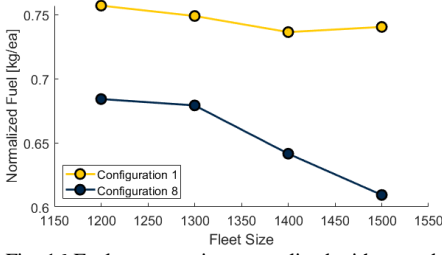


Fig. 16 Fuel consumption normalized with served customer amount

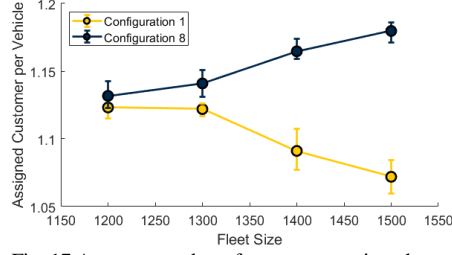


Fig. 17 Average number of customers assigned per running vehicle

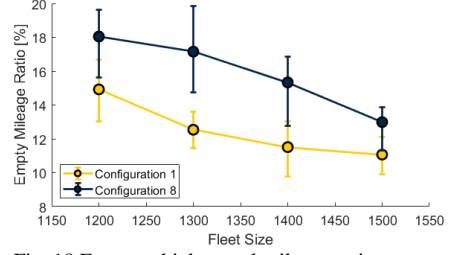


Fig. 18 Empty vehicle travel mileage ratio

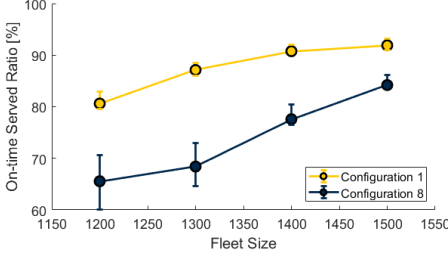


Fig. 19 Customer served within travel time constraints

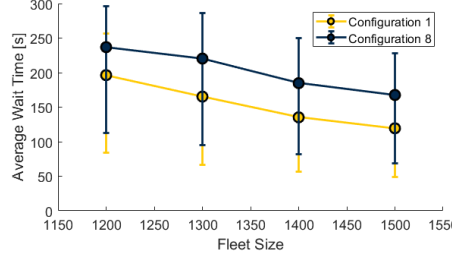


Fig. 20 Average wait time

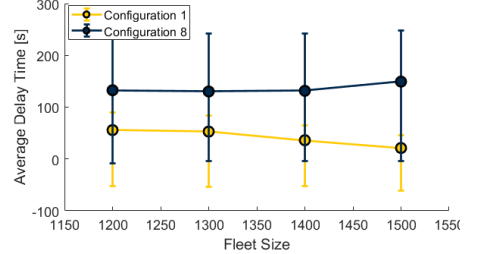


Fig. 21 Average delay time

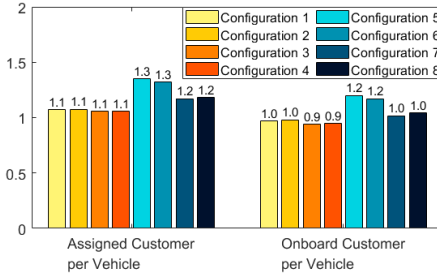


Fig. 22 MOD algorithm performance comparison — average customer assigned and onboard of each vehicle

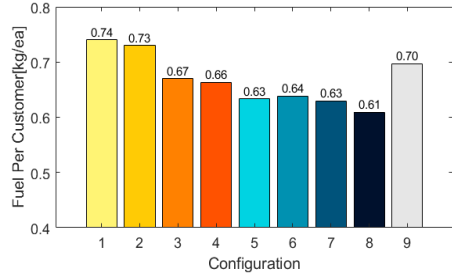


Fig. 23 Fuel Consumption per Customer

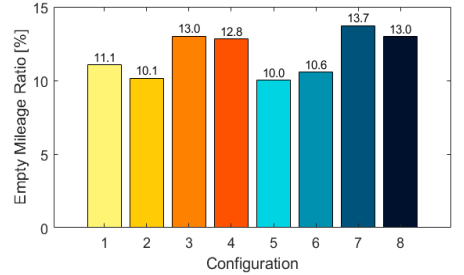


Fig. 24 Empty travel distance ratio

Availability as a function of fleet size using both shortest time routing and eco-routing is shown in Fig. 15. Due to the lower average speed results from the eco-routing strategy, more vehicles are required to achieve the same availability compared with the shortest time routing. Under the assumptions of queuing network based formulation, to achieve more than 95% availability for all partitions, 1,321 vehicles are required using the eco-routing strategy, and 1,134 vehicles are required using the shortest time routing strategy.

Numerical simulations are used for performance evaluation using different fleet sizes given a max wait time of 5 minutes and a max delay time of 5 minutes for configuration 1 and configuration 8. The fleet performance is summarized from Fig. 16 to Fig. 21, where 25th and 75th percentiles are represented using error bars. The fuel oriented configuration (configuration 8) consumes less fuel compared with the travel time oriented configuration (configuration 1) as shown in Fig. 16. Due to the fleet cost oriented objective function in the assignment step, the average number of customers per vehicle is higher for configuration 8, indicating more trips are shared. However, the average wait time and delay time of configuration 8 are longer than configuration 1 for all fleet sizes, and fewer customers are served within their travel time constraints (Fig. 19). For all configurations, the ratio of customers served within time constraints increases with the fleet size. For configuration 1, 1,200 vehicles can serve more than 80% of the customers within the time constraints, while 1,500 vehicles are required for

configuration 8. In the following sections, the fleet size is set to be 1,500.

D. MOD and Routing Strategy's Influence on Energy

The main goal of the simulations is to assess the impact of different routing strategies on the fleet fuel consumption. In this Section, we fix the demand ratio served by the MOD fleet at 4% of the total demand during the weekdays from 17:00 to 19:00. The simulated data from 18:00 ~ 19:00 is used for evaluation after the system reaches steady-state. The fleet size is 1,500, which is necessary to serve 80% of the customers within their travel time constraints for all configurations. This means the fleet size is larger than necessary for some configurations. However, when the vehicles are not dispatched, they incur neither time nor fuel cost, and thus will not affect the final performance measures. The performance of shareability is shown in Fig. 22. it can be seen that when the fleet cost is minimized, more shared trips are selected, and the average number of assigned customer per vehicle increases from 1.1 to 1.3, and the average number of onboard customers per vehicle increases from 1 to 1.2, indicating that more trips are shared and empty vehicle miles is reduced. However, due to the difference in the origin and destination distributions as well as the lower trip average speed, more rebalance trips are assigned for which no shared trips are allowed when eco-routing is applied. The increased amount of the rebalance trips reduced the average number of customers assigned per vehicle from 1.3 to 1.2 and

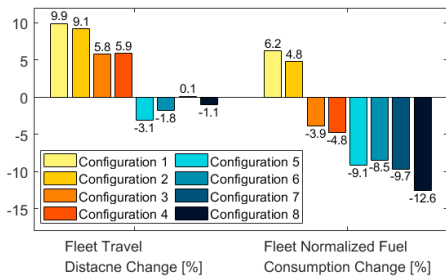


Fig. 25 Change in fleet total travel distance and fuel consumption per customer

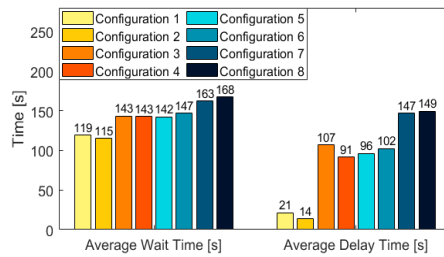


Fig. 26 Time Performance Comparison of Configurations

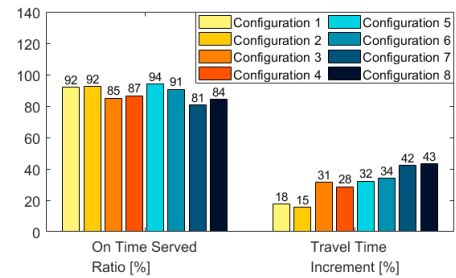


Fig. 27 Ratio of customers served within travel time constraints

the number of onboard customers from 1.2 to 1 when the assignment objective is the fleet fuel consumption.

The performance in fuel consumption and vehicle mileage are summarized in Fig. 23 to Fig. 25. When the objective function of the trip assignment is travel time and the shortest time routing strategy is used, the fuel consumption per customer is increased by 6.2% compared with the baseline when every trip uses a personal vehicle. Use eco-routing for unoccupied vehicles can reduce fuel usage per customer served by 1.3%, but still consumes 4.8% more fuel compared with the baseline. However, if the objective function is to minimize the fleet fuel consumption, the fuel consumption per customer can be reduced by 9% to 12% compared with the baseline.

The results indicate that the shared-rides can reduce the trip fuel consumption by 12%, but if the fleet is not properly operated, the total fuel consumption can increase. The results also indicate that with the same objective function, using eco-routing for trips can further reduce fuel consumption by 10% if the trip assignment objective is travel time, and 4% if the trip assignment objective is fleet fuel consumption compared with the configurations that using the fastest route. When fleet fuel is optimized, using eco-routing reduces average travel speed, making the additional benefit to fuel consumption limited.

The travel time performance is summarized in Fig. 26 and Fig. 27. Since the wait time and delay time of customers are modeled as constraints for trip assignment, all configurations can serve more than 80% of the customers within the travel time constraints. As shown in the plots, shared mobility has the potential to reduce the total fuel consumption but can increase travel time. The objective function can also be defined as a weighted sum of individual benefit and system benefit, and parametric study can be used to find the Pareto optimal points.

VII. CONCLUSIONS

A Bayesian nonparametric data-driven fuel consumption model is developed to estimate fuel cost for route optimization. Using the model, an Eco-MOD fleet assignment framework is developed to minimize fleet fuel consumption while satisfying travel time constraints. The system is evaluated using SUMO calibrated with real-world driving data. The algorithm shows the potential to reduce fleet fuel consumption while serving more than 80% of the customers within their travel time constraints.

VIII. ACKNOWLEDGMENT

The authors would like to thank the University of Michigan Transportation Research Institute (UMTRI) for making the data from the Safety Pilot Model Deployment (SPMD) project

available. This work is sponsored by the U.S. Department of Energy Vehicle Technologies Office under the award DE-EE0007212, an initiative of the Energy Efficient Mobility Systems Program. David Anderson, a Department of Energy Office of Energy Efficiency and Renewable Energy manager, played an important role in establishing the project concept, advancing implementation, and providing ongoing guidance.

REFERENCES

- [1] EIA, "Annual Energy Outlook 2017 with projections to 2050," pp. 1–64, 2017.
- [2] D. Schrank, B. Eisele, T. Lomax, and J. Bak, "2015 Urban Mobility Scorecard," *Texas A&M Transp. Institute*, vol. 39, no. August, p. 5, 2015.
- [3] X. Huang and H. Peng, "Eco-Routing based on a Data Driven Fuel Consumption Model," in *14th International Symposium on Advanced Vehicle Control (AVEC)*, 2018.
- [4] A. Rousseau, P. Sharer, and F. Besnier, "Feasibility of Reusable Vehicle Modeling: Application to Hybrid Vehicles," *SAE Tech. Pap.*, no. 2004-01-1618, p. 12, 2004.
- [5] H. Rakha, K. Ahn, and A. Trani, "Development of VT-Micro model for estimating hot stabilized light duty vehicle and truck emissions," *Transp. Res. Part D Transp. Environ.*, 2004.
- [6] F. Calise, A. Palombo, and L. Vanoli, "Design and partial load exergy analysis of hybrid SOFC-GT power plant," *J. Power Sources*, 2006.
- [7] W. Hasewend, "AVL CRUISE," *ATZ - Automob. Zeitschrift*, 2001.
- [8] J. Kwon, A. Rousseau, and P. Sharer, "Analyzing the uncertainty in the fuel economy prediction for the EPA MOVES binning methodology," *SAE Int.*, 2007.
- [9] J. Koupal, M. Cumberworth, H. Michaels, M. Beardsley, and D. Brzezinski, "Design and Implementation of MOVES: EPA's New Generation Mobile Source Emission Model," *Int. Emiss. Invent. Conf.*, 2003.
- [10] S. K. Zegeye, B. De Schutter, H. Hellendoorn, and E. Breunese, "Model-based traffic control for balanced reduction of fuel consumption, emissions, and travel time," in *IFAC Proceedings Volumes (IFAC-PapersOnline)*, 2009.
- [11] H. Rakha, K. Yue, and F. Dion, "VT-Meso model framework for estimating hot-stabilized light-duty vehicle fuel consumption and emission rates," *Can. J. Civ. Eng.*, 2011.
- [12] X. Qi and Y. Zhang, "Data-Driven Macroscopic Energy Consumption Estimation for Electric Vehicles with Different Information Availability," in *Proceedings - 2016 International Conference on Computational Science and Computational Intelligence, CSCI 2016*, 2017.
- [13] K. Boriboonsomsin, M. Barth, S. Member, W. Zhu, and A. Vu, "ECO-Routing Navigation System based on Multi-Source Historical and Real-Time Traffic Information," *Network*, vol. 13, no. 4, pp. 1694–1704, 2012.
- [14] M. Kubicka et al., "Performance of current eco-routing methods," *IEEE Intell. Veh. Symp. Proc.*, vol. 2016-Augus, pp. 472–477, 2016.
- [15] E. Yao and Y. Song, "Study on Eco-Route Planning Algorithm and Environmental Impact Assessment," *J. Intell. Transp. Syst.*, vol. 17, no. 1, pp. 42–53, 2013.
- [16] M. Levin W. M. Duell, and S. Waller Travis, "Effect of Road Grade on Networkwide Vehicle Energy Consumption and Ecorouting," *Transp. Res. Rec. J. Transp. Res. Board*, no. 2427, p. pp 26–33, 2014.
- [17] W. Zeng, D. Candidate, T. Miwa, and T. Morikawa, "Application of machine learning and heuristic k- shortest path algorithm to eco-routing problem with travel time constraint," pp. 1–18, 2016.
- [18] M. Masikos, M. Theologou, K. Demestichas, and E. Adamopoulou,

- “Machine-learning methodology for energy efficient routing,” *IET Intell. Transp. Syst.*, 2014.
- [19] Y. Chen, L. Zhu, J. Gonder, S. Young, and K. Walkowicz, “Data-driven fuel consumption estimation: A multivariate adaptive regression spline approach,” *Transp. Res. Part C Emerg. Technol.*, vol. 83, pp. 134–145, 2017.
 - [20] Y. Nie and Q. Li, “An eco-routing model considering microscopic vehicle operating conditions,” *Transp. Res. Part B Methodol.*, vol. 55, pp. 154–170, 2013.
 - [21] A. Elbery, H. Rakha, M. Y. ElNainay, W. Drira, and F. Filali, “Eco-routing: An Ant Colony based Approach,” *Proc. Int. Conf. Veh. Technol. Intell. Transp. Syst.*, no. June, pp. 31–38, 2016.
 - [22] J. Sun and H. X. Liu, “Stochastic Eco-routing in a Signalized Traffic Network,” *Transp. Res. Procedia*, vol. 7, pp. 110–128, 2015.
 - [23] T. S. Stephens, J. Gonder, Y. Chen, Z. Lin, C. Liu, and D. Gohlke, “Estimated Bounds and Important Factors for Fuel Use and Consumer Costs of Connected and Automated Vehicles Estimated Bounds and Important Factors for Fuel Use and Consumer Costs of Connected and Automated Vehicles,” no. November, 2016.
 - [24] “Shared Mobility On The Road Of The Future.” [Online]. Available: <https://www.forbes.com/sites/morganstanley/2016/07/20/shared-mobility-on-the-road-of-the-future/#a3a6c851cae8>. [Accessed: 20-Mar-2019].
 - [25] C. D. Porter, A. Brown, J. DeFlorio, E. McKenzie, W. Tao, and L. Vimmerstedt, “Effects of travel reduction and efficient driving on transportation: Energy use and greenhouse gas emissions,” 2013.
 - [26] J. Alonso-mora, A. Wallar, and D. Rus, “Predictive Routing for Autonomous Mobility-on-Demand Systems with Ride-Sharing,” pp. 3583–3590, 2017.
 - [27] J. Alonso-Mora, S. Samaranayake, A. Wallar, E. Frazzoli, and D. Rus, “On-demand high-capacity ride-sharing via dynamic trip-vehicle assignment,” *Proc. Natl. Acad. Sci.*, vol. 114, no. 3, pp. 462–467, Jan. 2017.
 - [28] F. Miao *et al.*, “Taxi Dispatch with Real-Time Sensing Data in Metropolitan Areas: A Receding Horizon Control Approach,” *IEEE Trans. Autom. Sci. Eng.*, vol. 13, no. 2, pp. 463–478, 2016.
 - [29] F. Rossi, R. Zhang, and M. Pavone, “Congestion-Aware Randomized Routing in Autonomous Mobility-on-Demand Systems,” *Transp. Res. Part B Methodol.*, vol. 99, pp. 1–29, Sep. 2016.
 - [30] R. Zhang, F. Rossi, and M. Pavone, “Analysis, Control, and Evaluation of Mobility-on-Demand Systems: a Queueing-Theoretical Approach,” pp. 1–10, 2018.
 - [31] K. Treleven, M. Pavone, and E. Frazzoli, “Models and Asymptotically Optimal Algorithms for Pickup and Delivery Problems on Roadmaps (submitted),” *Decis. Control (CDC), 2012 51st IEEE Conf.*, pp. 5691–5698, 2012.
 - [32] M. Čáp, S. Vajna, and E. Frazzoli, “Fleet Sizing in Vehicle Sharing Systems with Service Quality Guarantees,” 2018.
 - [33] A. Wallar, J. Alonso-mora, and D. Rus, “Optimizing Vehicle Distributions and Fleet Sizes for Mobility-on-Demand,”
 - [34] M. M. Vazifeh, P. Santi, G. Resta, S. H. Strogatz, and C. Ratti, “Addressing the minimum fleet problem in on-demand urban mobility,” *Nature*, vol. 557, no. 7706, pp. 534–538, May 2018.
 - [35] R. Tachet *et al.*, “Scaling Law of Urban Ride Sharing,” *Sci. Rep.*, vol. 7, p. 42868, 2017.
 - [36] S. Shaheen and E. Martin, “Impacts of car2go on Vehicle Ownership, Modal Shift, Vehicle Miles Traveled, and Greenhouse Gas Emissions,” pp. 0–25, 2016.
 - [37] D. J. Bertsimas and D. Simchi-Levi, “A New Generation of Vehicle Routing Research: Robust Algorithms, Addressing Uncertainty,” *Oper. Res.*, vol. 44, no. 2, pp. 286–304, 1996.
 - [38] E. Lam and P. Van Hentenryck, “A branch-and-price-and-check model for the vehicle routing problem with location congestion,” *Constraints*, vol. 21, no. 3, pp. 394–412, 2016.
 - [39] R. W. Bent and P. Van Hentenryck, “Scenario-Based Planning for Partially Dynamic Vehicle Routing with Stochastic Customers,” *Oper. Res.*, vol. 52, no. 6, pp. 977–987, 2004.
 - [40] A. Maheo, P. Kilby, and P. Van Hentenryck, “Benders Decomposition for the Design of a Hub and Shuttle Public Transit System,” no. January 2018, 2015.
 - [41] G. Laporte, “The vehicle routing problem: An overview of exact and approximate algorithms,” *Eur. J. Oper. Res.*, 1992.
 - [42] N. Agatz, A. Erera, M. Savelsbergh, and X. Wang, “Optimization for dynamic ride-sharing: A review,” *Eur. J. Oper. Res.*, vol. 223, no. 2, pp. 295–303, 2012.
 - [43] W. Herbawi and M. Weber, “A Genetic and Insertion Heuristic Algorithm for Solving the Dynamic Ridematching Problem with Time Windows,” *Gecco 2012*, pp. 385–392, 2012.
 - [44] M. M. Solomon, “Algorithms for the vehicle routing and scheduling problems with time window constraints,” vol. 35, no. 2, pp. 254–265, 1987.
 - [45] D. Teodorović and M. Dell’orco, “Bee Colony Optimization – A cooperative learning approach to complex transportation problems,” *Adv. OR AI Methods Transp.*, 2015.
 - [46] N. Masoud and R. Jayakrishnan, “A decomposition algorithm to solve the multi-hop Peer-to-Peer ride-matching problem,” *Transp. Res. Part B Methodol.*, vol. 99, no. May, pp. 1–29, May 2017.
 - [47] H. Hosni, J. Naoum-Sawaya, and H. Artail, “The shared-taxi problem: Formulation and solution methods,” *Transp. Res. Part B Methodol.*, vol. 70, pp. 303–318, 2014.
 - [48] P. Santi, G. Resta, M. Szell, S. Sobolevsky, S. H. Strogatz, and C. Ratti, “Quantifying the benefits of vehicle pooling with shareability networks,” *Proc. Natl. Acad. Sci.*, vol. 111, no. 37, pp. 13290–4, 2014.
 - [49] T. Zhou, C. Osorio, and E. Fields, “A data-driven discrete simulation-based optimization algorithm for large-scale two-way car-sharing network design.”
 - [50] A. Prorok and V. Kumar, “Privacy-Preserving Vehicle Assignment for Mobility-on-Demand Systems,” 2017.
 - [51] M. W. Levin, “Congestion-aware system optimal route choice for shared autonomous vehicles,” *Transp. Res. Part C Emerg. Technol.*, vol. 82, pp. 229–247, 2017.
 - [52] R. Zhang, F. Rossi, and M. Pavone, “Model Predictive Control of Autonomous Mobility-on-Demand Systems,” *Int. Conf. Robot. Autom.*, pp. 1382–1389, 2016.
 - [53] M. Cap and J. Alonso-Mora, “Multi-Objective Analysis of Ridesharing in Automated Mobility-on-Demand,” 2018.
 - [54] S. Erdoğan and E. Miller-Hooks, “A Green Vehicle Routing Problem,” *Transp. Res. Part E Logist. Transp. Rev.*, vol. 48, no. 1, pp. 100–114, 2012.
 - [55] J. Auld, M. Hope, H. Ley, V. Sokolov, B. Xu, and K. Zhang, “POLARIS: Agent-based modeling framework development and implementation for integrated travel demand and network and operations simulations,” *Transp. Res. Part C Emerg. Technol.*, vol. 64, pp. 101–116, 2016.
 - [56] D. Bezzina and J. Sayer, “Safety pilot model deployment: Test conductor team report,” *Rep. No. DOT HS*, vol. 812, no. June, p. 171, 2014.
 - [57] D. Krajzewicz and J. Erdmann, “Recent Development and Applications of SUMO–Simulation of Urban Mobility,” *Int. J. ...*, vol. 5, no. 3, pp. 128–138, 2012.
 - [58] C. M. Bishop, *Pattern Recognition and Machine Learning*. Springer, 2006.
 - [59] D. M. Blei, A. Kucukelbir, and J. D. McAuliffe, “Variational Inference: A Review for Statisticians,” *J. Am. Stat. Assoc.*, vol. 112, no. 518, pp. 859–877, 2017.
 - [60] C. Bron and J. Kerbosch, “Algorithm 457: finding all cliques of an undirected graph,” *Commun. ACM*, vol. 16, no. 9, pp. 575–577, 1973.
 - [61] S. Ma, Y. Zheng, and O. Wolfson, “Real-Time City-Scale Taxi Ridesharing,” *IEEE Trans. Knowl. Data Eng.*, vol. 27, no. 7, pp. 1782–1795, 2015.
 - [62] G. O. Inc., “Gurobi Optimizer reference manual,” *Www.Gurobi.Com*, vol. 6, p. 572, 2014.
 - [63] J. Auld and A. K. Mohammadian, “Activity planning processes in the Agent-based Dynamic Activity Planning and Travel Scheduling (ADAPTS) model,” *Transp. Res. Part A Policy Pract.*, 2012.
 - [64] A. F. Acosta, J. E. Espinosa, and J. Espinosa, “TraCI4Matlab: Enabling the integration of the SUMO road traffic simulator and Matlab® through a software re-engineering process,” in *Lecture Notes in Control and Information Sciences*, 2015.
 - [65] M. Maciejewski, “A Comparison of Microscopic Traffic Flow Simulation,” *Transp. Probl.*, vol. 5, no. 4, 2010.
 - [66] X. Huang and H. Peng, “Efficient Mobility-on-Demand System with Ride-Sharing,” in *IEEE Conference on Intelligent Transportation Systems, Proceedings, ITSC*, 2018.
 - [67] Y. Gal and Z. Ghahramani, “Dropout as a Bayesian Approximation: Representing Model Uncertainty in Deep Learning,” *Nurs. Clin. North Am.*, vol. 14, no. 1, pp. 145–56, Jun. 2015.
 - [68] A. Kendall and Y. Gal, “What Uncertainties Do We Need in Bayesian Deep Learning for Computer Vision?,” no. Nips, 2017.
 - [69] K. Ballantyne *et al.*, “Toward a Systematic Approach to the Design and Evaluation of Automated Mobility-on-Demand Systems: A Case Study in Singapore,” pp. 0–16, 2014.

[70] M. Pavone, S. L. Smith, E. Frazzoli, and D. Rus, "Robotic load balancing for mobility-on-demand systems The," pp. 0–25, 2012.



Xianan Huang received the Ph.D degree in mechanical engineering from University of Michigan, Ann Arbor, MI, USA, in 2019. From 2013 to 2014 he was an undergraduate researcher at Purdue University. Since 2014 he has been a graduate researcher at University of Michigan, Ann Arbor. His research interests include connected automated vehicle,

intelligent transportation system, statistical learning and controls. Dr. Huang's awards and honors include A-Class scholar of Shanghai Jiaotong University and Summer Undergraduate Research Fellowship (Purdue University).



Boqi Li received his B.S. degree in Mechanical Engineering at the University of Illinois at Urbana-Champaign. He received his M.S. degree at Stanford University. He is currently a Ph.D. student at the University of Michigan at Ann Arbor. His research interests include eco-routing, reinforcement learning, and cooperative control of connected and

automated vehicles.



Hui Peng received the Ph.D. degree from the University of California, Berkeley, CA, USA, in 1992. He is currently a Professor with the Department of Mechanical Engineering, University of Michigan, Ann Arbor. He is currently the U.S. Director of the Clean Energy Research Center—Clean Vehicle Consortium, which supports 29 research projects

related to the development and analysis of clean vehicles in the U.S. and in China. He also leads an education project funded by the Department of Energy to develop ten undergraduate and graduate courses, including three laboratory courses focusing on transportation electrification. He serves as the Director of the University of Michigan Mobility Transformation Center, a center that studies connected and autonomous vehicle technologies and promotes their deployment. He has more than 200 technical publications, including 85 in refereed journals and transactions. His research interests include adaptive control and optimal control, with emphasis on their applications to vehicular and transportation systems. His current research focuses include design and control of electrified vehicles and connected/automated vehicles.



Joshua Auld is a Principal Computational Transportation Engineer in Argonne's Vehicle and Mobility Systems Group, and technical manager of transportation systems simulation. He completed his Doctorate in August 2011, in the Civil and Materials Engineering Department of the University of Illinois at Chicago with a concentration in transportation.

Dr. Auld has experience in a variety of areas in transportation, with a primary focus on dynamic activity-based travel demand models and the interactions between travel demand and intelligent transportation systems operations. He has over 40 publications in refereed journals and books. He is a member of the TRB Travel Forecasting Resource and Transportation Demand Forecasting Committees.



Vadim Sokolov received his Ph.D. degree in mathematics from Northern Illinois University in 2008. He is currently an assistant professor in the Systems Engineering and Operations Research Department at George Mason University. He has more than 30 publications in refereed journals and transactions. His research interests include deep learning, Bayesian

analysis of time series data, design of computational experiments. Inspired by an interest in urban systems he co-developed mobility simulator called Polaris that is currently used for large scale transportation networks analysis by both local and federal governments. Prior to joining GMU he was a principal computational scientist at Argonne National Laboratory, a fellow at the Computation Institute at the University of Chicago and lecturer at the Master of Science in Analytics program at the University of Chicago.